DYNAMIC TRANSFER OF ROBUST AMB CONTROLLERS

Guoxin Li, Paul E. Allaire
Department of Mechanical and Aerospace Engineering, University of Virginia
Charlottesville, VA 22903, USA. Email: gl2n, pea@virginia.edu

Zongli Lin, Bin Huang
Department of Electrical and Computer Engineering, University of Virginia
Charlottesville, VA 22903, USA. Email: zl5y, bh4h@virginia.edu

ABSTRACT

This paper studies dynamic controller switching in active magnetic bearing (AMB) supported high speed gyroscopic rotor systems. To control a gyroscopic rotor over a wide speed range, a single linear time invariant (LTI) controller is often not adequate due to the speed-dependent system characteristics and the high robustness requirement. One approach is to design several controllers for each segment of speed range and switch between controllers. Dynamic transfer of different controllers play an important role in this piecewise robust control design method. The bumpless transfer problem will be introduced and analyzed. A bidirectional bumpless transfer scheme based on the robust observer concept is proposed to address the controller transient switching problem. To implement this scheme, several important computational issues are addressed. The proposed approach is successfully implemented on an AMB control test rig.

Keywords: Active magnetic bearings, gyroscopic effects, robust control, bumpless transfer, real-time systems

1 INTRODUCTION

Active magnetic bearings (AMBs) offer many advantages over traditional bearings, such as higher attainable speeds, lower power consumption, active vibration control capability, no lubrication and no wear. However, AMB systems are open loop unstable. Therefore, feedback control is required. Conventional control systems applied to magnetic bearings in previous applications often assume that the rotor-AMB system is linear and time invariant. Unfortunately, the rotor-AMB system dynamic characteristics are inherently speed dependent and nonlinear. In a number of high speed rotor applications such as high inertia flywheel systems, the speed dependent characteristics such as gyroscopics effects cannot be neglected. Currently, a vast majority of AMB controllers are designed using linear system theory. The plant dynamics are linearized around the operating point, and the system stability and performance are only guaranteed in the neighborhood of equilibrium points. A single LTI controller often cannot even stabilize the system over the entire operating speed range. To run such a system over a wide operating speed range, switching type linear controllers or gain scheduled controllers are often suggested. In addition, optimal control often results in a switching type of controller. Switching controllers may experience a bump due to the unknown initial conditions of the off-line controller. This prohibits its use in high speed rotor applications where the vibrations should not exceed certain limits. At the switching point, it is highly desirable that the system transfers from one controller to another without introducing large transient vibrations of the rotor. The objective of this paper is to provide a practical technique to avoid transient vibrations.

The remainder of this paper is organized as follows. The bumpless transfer problem is first introduced in Section 2. The observer based approach to bumpless transfer design is developed. In Section 3, several important implementation issues are addressed and testing results are presented. Finally, conclusions are drawn in Section 4.

2 BUMPLESS TRANSFER DESIGN

The motivation of this study comes from the control of flywheel energy storage systems. For the high speed flywheel, the rotor is often flexible and the dynamic equation of motion in the lateral direction takes the following form

$$M_r\ddot{x}_r + (D_r + \omega G_r)\dot{x}_r + (K_r + \omega D_i + \frac{1}{2}\dot{\omega}G_r + \omega^2 K_\omega)x_r = f_r(t) \quad (1)$$

where ω is the rotation speed, x_r contains the translational and rotational degrees of freedom in the two lateral directions, M_r, K_r represent the rotor mass, stiffness model, D_r and D_i represent structural damping and internal damping in the rotor, the matrix G_r contains the gyroscopic coeffiecients, and K_ω represents the centrifugal stiffening effect. Matrices G_r and D_i are skew symmetric. The magnetic bearing dynamics is incorporated into $f_r(t)$. The vector $f_r(t)$ also contains the unbalance forces and disk skew effects as well as the disturbance forces.

For flywheel systems operating over a wide speed range, two dominant issues must be addressed in the control design. One is the high robustness requirement and the other is the control of the speed dependent dynamics such as the gyroscopic effects, internal damping and centrifugal stiffening effects. Advanced multi-variable robust optimal control, especially μ-synthesis, provides a systematic tool to achieve the robustness. To address the speed dependent dynamics, currently, there are two important approaches. One is the so-called piecewise μ synthesis proposed in [11]. The other is gain scheduled control, in particular, the linear parameter varying (LPV) approach [14, 17]. In the LPV controller design, the stability and performance requirement are characterized in terms of linear matrix inequalities (LMIs), the gain-scheduling problem is solved using the interior point methods. High order LPV controllers are very difficult to implement with currently available computational resources. In the more practical piecewise μ synthesis method, the speed dependent dynamics are treated as time varying uncertainties, and the system is represented in linear fraction transformation (LFT) form. The operating speed range is divided into several regions where the gyroscopic effects do not vary significantly. Several controllers are then designed for each speed region. The overall controller is implemented by switching between regional controllers as the speed varies from one region to another. During the switching of controllers, the stability is guaranteed. However, a transient vibration of large amplitude may occur due to the unknown controller initial conditions. Furthermore, if the vibration amplitude is too high, robustness is always a concern since the model for control synthesis is based on small vibration amplitudes near the equilibrium point. The AMB amplifiers may become saturated, and the system may lose stability.

Traditionally, the bumpless transfer problem refers to the instantaneous switching between manual and automatic control of a process while retaining a smooth control signal. Many different techniques have been developed [4]. Most of these techniques are presented in the context of anti-windup design. In general, the bumpless transfer problem can be treated as a tracking problem. Two of the most well known techniques for bumpless transfer design are conditioning techniques [5] and observer based techniques [1]. The fundamental idea of the conditioning technique is to manipulate the reference signal such that the off-line controller output is in agreement with the on-line controller signal. The observer based approach is to adjust the off-line controller's initial states in order to guarantee the continuity of control output signal at the switching. A general framework that encompasses most of the anti-windup and bumpless transfer schemes is presented in [2, 9]. A comprehensive study of these schemes can be found in [3].

Many of the bumpless transfer techniques are developed and applied for low order process controllers. There are not many published implementation results for switching higher order controllers. To the best of our knowledge, no switching techniques and experimental results are published in the magnetic bearing community especially for high speed applications. In this paper, a switching technique was developed based on the observer concept to address the AMB controller transient switching problem.

The objective of bumpless transfer is to obtain the instantaneous switching between controllers while retaining a smooth rotor vibration. Generally, rotor-AMB systems can be modeled as linear parameter varying systems using state space realization. The plant dynamics can be represented as

$$\begin{aligned} \dot{q}(t) &= A_p(\omega)q(t) + B_p u(t), \\ z(t) &= C_p q(t), \end{aligned} \tag{2}$$

where $q(t)$ is the state variable, $u(t)$ is the control signal and $z(t)$ is the output signal. The LTI controllers may take the following state space form

$$\begin{aligned} \dot{\eta}(t) &= A_c\eta(t) + B_c z(t), \\ u(t) &= C_c\eta(t). \end{aligned} \tag{3}$$

Intuitively, according to the above plant dynamic equations, to ensure the bumpless rotor transient vibration during the controller switching, the control signal of the off-line controller must be "synchronized" with the on-line controller. Mathematically, this can be guaranteed by requiring the two controllers output and their derivatives to be close enough at the switching time t_s, i.e.,

$$u_2(t_s) \approx u_1(t_s), \quad \frac{d^k u_2(t)}{dt^k}|_{t=t_s} \approx \frac{d^k u_1(t)}{dt^k}|_{t=t_s}, \quad k = 1, 2, \ldots. \tag{4}$$

Generally, it is difficult to know the off-line controller states at the switching point because the off-line controller is not controlling the system before the switching occurs. For lower order systems, with a band pass filter to approximate the derivatives, the states of the off-line controller may be computed by the above switching conditions. Since the sensor output signal in magnetic bearing systems is noise sensitive, and the robust controller order is generally large, it is not possible to do the direct computation. In practice, the plant output $z(t)$ and the on-line controller output $u(t)$ can be accessed before the switching. The idea is to cause the off-line controller tracking the $u(t)$ over a certain period of time before the switching. Then at the switching point, the control signal $u(t)$ is smooth. This can be achieved by an observer.

A suitable bumpless transfer scheme for high speed rotor-AMB systems should have the following properties. First, it must be robust. In a high speed application, the rotor-AMB is always subjected to many different sources of disturbance. The system is parameter dependent, and acceleration and deceleration will change the system dynamics. Second, it must be bidirectional. The rotor may speed up and slow down during the operation. Third, it must handle high acceleration or deceleration rates. The plant dynamics are in the transient stages. The tracking response should be fast enough. Finally, the computation should not be too expensive. It should be implemented for high order controllers with the available hardware. To meet the above requirement, a practical bumpless transfer scheme is developed for rotor-AMB system as shown in Fig. 1. As a general

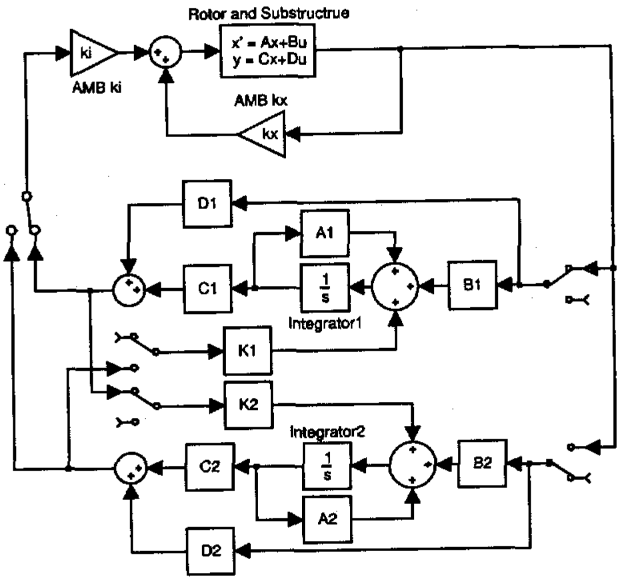

Figure 1: The bumpless transfer diagram.

tracking control problem, K_1 and K_2 can be designed to track the on-line controller output $u(t)$. The controller transfer is bidirectional with K_1 and K_2. If the off-line controller is taken to be the same as the on-line controller, the tracking scheme is exactly an observer. The Kalman filter concept is employed in our design to estimate the states of the off-line controller due to its robust properties in the presence of noise. When the rotor speed is approaching to the switching speed, for example, reaching 95% of the switching speed, the switches for off-line controller and the observer gain are engaged. The observer starts to track the controller output signal $u(t)$ with input $z(t)$. At the switching point, the off-line controller is switched into the line and observer gain K is cut off. The off-line controller states obtain the desired value for smooth transition.

Consider the controller as a stochastic LTI system

$$\begin{aligned} \dot{\eta}(t) &= A_c\eta(t) + B_c z(t) + L\xi(t), \\ u(t) &= C_c\eta(t) + \theta(t), \end{aligned} \tag{5}$$

where $\xi(t)$ and $\theta(t)$ are assumed to be white Gaussian noise with zero mean, i.e.,

$$E\{\xi(t)\xi^T(\tau)\} = \Xi\delta(t-\tau), E\{\theta(t)\theta^T(\tau)\} = \Theta\delta(t-\tau), \tag{6}$$

the observer gets the input $z(t)$, $u(t)$, and generates the optimal estimates $\hat{u}(t)$, $\hat{\eta}(t)$ by the observer dynamic equation

$$\begin{aligned} \dot{\hat{\eta}}(t) &= A_c\hat{\eta}(t) + B_c z(t) + K(t)[u(t) - C_c\hat{\eta}(t)], \\ \hat{u}(t) &= C_c\hat{\eta}(t). \end{aligned} \tag{7}$$

The Kalman filter gives the optimal estimation of state in terms of mean square errors [8]. When the rotor operates in transient acceleration, an optimal Kalman gain is not constant. Since the rotor acceleration rate is relatively low compared to the sampling rate, a constant asymptotic value of the Kalman filter gain is utilized for implementation purposes. If the rotor acceleration and deceleration rates are very high in some applications, we may consider a gain scheduling method, i.e., varying Kalman gain during the observation. Since the rate of change of the Kalman gains is slow compared to the sampling rate, each value of Kalman gain may be used for a part of observation time. In any case, the Kalman gain computation can be performed off-line. This requires the solution of the steady state algebraic Riccati equation,

$$A_c\Sigma + \Sigma A_c^T + L\Xi L^T - \Sigma C_c^T\Theta^{-1}C_c\Sigma = 0, \tag{8}$$

and the Kalman gain is determined by

$$K = \Sigma C_c^T\Theta^{-1}. \tag{9}$$

For digital control implementation, the $u(t)$ signal can be obtained accurately. In the case of exact measurements, i.e., noise intensity Θ approaches zero, the Kalman filter yields exact state estimates for the minimum phase plant [10]. Since robust controllers is not necessarily minimum phase, the state estimation may not be perfect.

3 IMPLEMENTATION

The UVa AMB control test rig was built to simulate a future flywheel energy storage system and serves as a platform for investigating different control schemes. The test rig consists of a rotor bearing assembly, a supporting frame and electronic control systems as illustrated in Fig. 2. The rotor is designed to be flexible in order to simulate the flexible shaft of the flywheel in very high speed applications. The rotor is suspended with two eight pole heteropolar radial magnetic bearings and one axial thrust magnetic bearing. The double acting thrust magnetic bearing, which supports the rotor vertically, is located at the top. Mechanical ball bearings with a clearance are employed as backup bearings. Differential eddy-current displacement probes are used to measure rotor's displacement. The design also incorporates the complete integration of the motor and rotor/shaft. The rotor bearing assembly is supported by a substructure frame. The frame is designed to be asymmetrical and flexible in order to simulate the space application environment. The system also includes anti-alias filters, the digital control, and amplifiers in its electronic loop as shown in Fig. 3, where V, A, N and M represent the control voltage, current, force and displacement respectively.

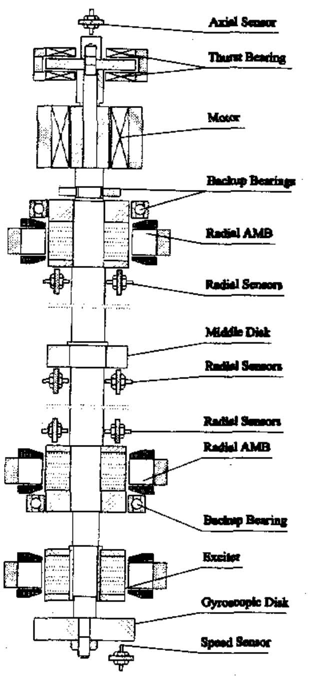

Figure 2: The schematic plot of the control test rig.

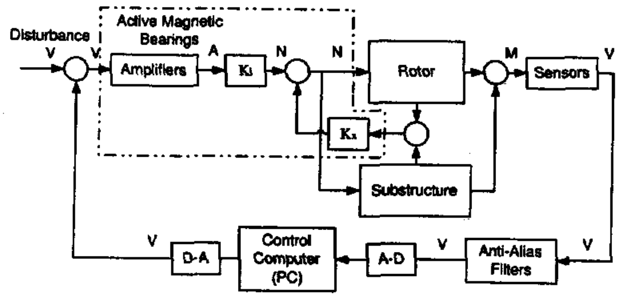

Figure 3: The block diagram of the flywheel test rig.

A Kalman observer provides optimal estimates of the controller states. However, the real-time computation for high order robust controllers is expensive. For some applications, such as flywheels in space applications, the computational resources are limited. The required real-time controller computation must not exceed the hardware limits. In addition, as the rotor runs at higher speed, a higher sampling rate is required. The real-time computation of a high order LTI controller and bumpless transfer scheme becomes an important issue. The discrete equation of the controller takes the form

$$\begin{aligned} \hat{\eta}(k+1) &= A_c\eta(k) + B_c z(k), \\ u(k) &= C_c\eta(k), \end{aligned} \qquad (10)$$

For a four input and four output system, the state update matrix calculation involves $2n^2 + 8n$ flops, and the output update requires another $8n$ flops, where n is the order of the controller. Since the most expensive computation is the $A_c(k)\eta(k)$, a certain structure of realization of $A_c(k)$ may be chosen to reduce the arithmetic and storage. For example, with the most desirable structure, i.e., real block diagonal structure, the computation of $A_c(k)\eta(k)$ reduces from $2n^2$ to $4n$ flops. For a 42th order controller, the computation of the sparse matrix controller at each sampling point reduces by a factor of 5 compared to that of a full matrix controller. We note that the flop counting is only a crude estimate of the actual computation time since it ignores subscripting, memory traffic and other overheads.

As we know, a matrix A_c is diagonalizable if and only if there is a set of n linearly independent eigenvectors. If A_c is diagonalizable, the real block diagonal structure can be obtained by a real similarity transformation. However, not all the real matrices are diagonalizable. A more general efficient form is the real Jordan canonical form. Each real matrix is similar to a block diagonal real matrix of the form [7]

$$\begin{bmatrix} C_{n1}(a_1,b_1) & \dots & 0 & 0 & \dots & 0 \\ \vdots & \ddots & \vdots & \vdots & & \vdots \\ 0 & \dots & C_{np}(a_p,b_p) & 0 & \dots & 0 \\ 0 & \dots & 0 & J_{nq}(\lambda_q) & \dots & 0 \\ \vdots & & \vdots & \vdots & \ddots & \vdots \\ 0 & \dots & 0 & 0 & \dots & J_{nr}(\lambda_r) \end{bmatrix}$$

where

$$C_k(a,b) = \begin{bmatrix} C(a,b) & I & \dots & 0 \\ 0 & C(a,b) & \dots & I \\ \vdots & \vdots & \ddots & I \\ 0 & 0 & \dots & C(a,b) \end{bmatrix},$$

and

$$C(a,b) = \begin{bmatrix} a & b \\ -b & a \end{bmatrix}.$$

In addition, for a real matrix, there is always a real non singular matrix T such that $T^{-1}A_cT$ is in real Jordan form. The controller state vector becomes $T\eta$, and the matrices B_c, C_c are transformed to $T^{-1}B_c$ and C_cT. Generally, computation of the Jordan form is numerically stiff. Care must be taken to check the numerical errors. We use the toolbox [13] for numerical computation. The transformation error is evaluated by $\|G_O - G_J\|_\infty$, where G_o and G_J represents the transfer function matrices of the original controller and its Jordan form. For our existing controllers, the transformation is numerically stable.

Several other measures are taken to alleviate the computation burden. First, from a scheduling point of view, the priority of the observer computation is lower than the on-line controller computation. The state update of the observer can be performed at a lower sampling rate in real-time implementation. Second, a mini-vector set of instructions are implemented. The Intel Pentium III processor contains a new set of instructions called Streaming SIMD (Single Instruction, Multiple Data) Extensions (SSE). The SSE instructions enable us to use instruction level parallelization which results in significant speedup [16]. Finally, A/D and D/A conversion sets another limitation for improving the computation performance. It is noticed that ISA cards are not suitable for high speed real-time control. We replaced our ISA A/D and D/A cards with the latest PCI card in order to obtain sufficiently fast conversion. After implementing all these measures, the sampling rate can reach 8000 Hz (125 ms) for 50th order controller at a 733 MHz Intel Pentium III processor while running one controller and one observer at the same time.

Because of the strong gyroscopic effects and the wide operational speed range, the piecewise μ design generates several controllers. Details of μ-synthesis controller design procedure are presented in [11, 15]. Each controller is effective in a range of speed. For example, Controller 1 and Controller 2 are designed based on the nominal speed at 10,000rpm and 15,000 rpm respectively, and each controller covers ±20% speed variation. The two controllers are designed to switch at 12,000 rpm. μ-synthesis design often results in large order controllers. First, the controller order must be reduced. Balanced model reduction is employed to reduce the controllers order from about 100th to 40th-50th, depending on the reduction error. The controllers are designed based on a continuous time model. For digital implementation, the reduced controllers are then discretized at chosen sampling rate using the Tustin method. The controllers are implemented on a 733MHz PC using RTic-Lab based on Real Time Linux [6]. The transient behavior during the switching is first tested. 8 KHz sampling rate is reached with a 48th order controller. As illustrated in Fig. 4, the rotor experienced $0.05mm$ $0-P$ vibration during the controller switching. The AMBs are nearly saturated. Fortunately, the controller is very robust, the system remains stable during switching.

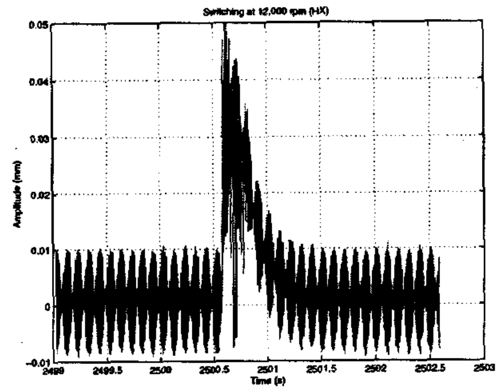

Figure 4: Controller transfer at 12,000 rpm without bumpless technique.

To design an observer, first, we analyze the output sensor signal to determine the noise covariance. The observer design must be robust to the disturbance and the noise. Discrete Kalman filters are designed for the switching controllers. The Kalman gain is determined and the observer dynamics are tested first. The test shows a good tracking property of the designed observer. The tracking error is within 10% as shown in a error percentage plot (Fig. 5). The settling time is about 1.5 seconds. The observer is engaged a few seconds before the switching. The switching scheme is first tested at lower speeds. Low speed controllers are designed. The switching is tested at 0 rpm, 4000 rpm, 6000 rpm, 7000 rpm, 8000 rpm. All the controller transfers are very smooth. The observer scheme is robust to the sensor noise and the disturbance. After the bumpless switching is obtained at low speeds, the switching is tested at 12,000 rpm above the first bending critical speed, i.e., 9500 rpm. As shown in Fig. 6, the switch is very smooth with bumpless transfer engaged at $t_s = 2477s$.

4 CONCLUSIONS

This paper presents an AMB controller switching technique for high speed applications. The motivation of this study comes from the piecewise control of a high speed rotor over a wide operating speed range. A robust observer is employed to obtain the off-line controller initial states. To reduce the computational cost, several measures are proposed and implemented. The switching scheme is successfully implemented on a high speed test rig. Smooth switching is obtained above the first bending critical speed. All the tests show that the proposed scheme is robust.

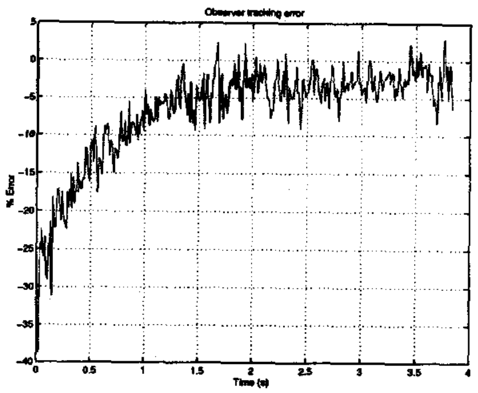

Figure 5: Observer tracking error.

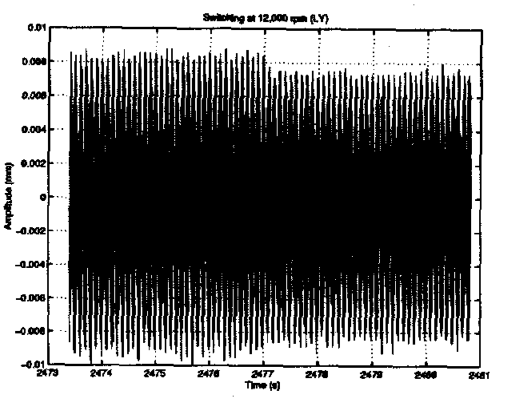

Figure 6: Controller transfer at 12,000 rpm with bumpless technique.

5 ACKNOWLEDGEMENTS

The authors wish to acknowledge that this research was supported by AFS Trinity Power Corporation as an independently funded continuation of research originally undertaken as a NASA, Goddard Space Flight Center, Small Business Innovative Research (SBIR) project.

References

[1] Åström, K. J. and Wittenmark, B. (1984) *Computer Controlled Systems, Theory and Design*, Prentice Hall, Englewood Cliffs, NJ, 2nd edition.

[2] Campo, P. J., Morari, M. and Nett, C. N. (1989). "Multivariable anti-windup and bumpless transfer: a general theory," *Proceedings of American Control Conference*, Pittsburgh, pp. 1706-1711.

[3] Edwards, C. and Postlethwaite, I. (1998). "Anti-windup and Bumpless-transfer schemes," *Automatica*, vol. 34, No. 2, pp. 199-210.

[4] Graebe, S. F. and Ahlen, A. (1995). "Bumpless Transfer," *The Control Handbook*, CRC Press pp. 381-381.

[5] Hanus, R., Kinnaert, M. and Henrotte, J.-L. (1987). "Conditioning technique, a general anti-windup and bumpless transfer method," *Automatica*, vol. 23, No. 6, pp. 729-739.

[6] Hilton, E. F., Humphrey, M., Stankovic, J. and Allaire, P. E. (2000). "Design of an open source, hard real time, controls implementation platform for active magnetic bearings", *Proceedings of the 7th Int. Symp. on Magnetic Bearings*, Zrich, Switzerland, pp. 329-334.

[7] Horn, A. R. and Johnson, R. C. (1985). *Matrix Analysis*, Cambridge University Press.

[8] Kalman, R. E. (1960). "A new approach to linear filtering and prediction problem," *ASME Journal of Basic Engineering*, vol. 82D, pp. 35-45.

[9] Kothare, V. M, Campo, P. J., Morari, M. and Nett, N. C. (1994). "A unified framework for the study of anti-windup designs," *Automatica*, vol. 30, No. 12, pp. 1869-1883.

[10] Kwakernaak, H. and Sivan, R. (1972). *Linear Optimal Control Systems*, J. Wiley & Sons, NewYork.

[11] Li, G., Lin, Z., Allaire, P. E., Huang, B., Jiang, W., Zorzi, S. E. and Bartlett, R. O. (2001). "Stabilization of a high speed rotor with active magnetic bearings by a piecewise μ-synthesis controller," *Proceedings of the 6th Int. Symp. on Magnetic Suspension Technology*, Turin, Italy, pp. 416-422.

[12] Li, G., Lin, Z., Allaire, P. E. and Luo, J. (2001). "Modeling of a high speed flywheel test rig with active magnetic bearings," submitted for publication.

[13] Lin, Z. and Chen, B. M. (1998). *Linear Systems Toolbox*, University of Virginia.

[14] Mason, S., Tsiotras, P. and Allaire, P.(1998). "Linear parameter varying controllers for flexible rotors supported on magnetic bearings," *Proceedings of the 6th Int. Symp. on Magnetic Bearings*, Cambridge, MA,USA, pp. 341-351.

[15] Schönhoff, U., Luo, J., Li, G., Hilton., E.F., Nordmann, R. and Allaire, P.E. (2000). "Implementation results of μ-synthesis control for an energy storage flywheel test rig," *Proceedings of the 7th Int. Symp. on Magnetic Bearings*, Zurich, Switzerland, August 2000.

[16] Skadron, K., Humphrey, M., Huang, B., Hilton, E., Luo, J. and Allaire, P. (2001). "Supporting higher-order controllers for magnetic bearings in a high-speed, real-time platform using general-purpose computers," *Proceedings of the 6th Int. Symp. on Magnetic Suspension Technology*, Turin, Italy, pp. 1-6.

[17] Zhang, H., Lin, Z., Allaire, P.E. and Huang, B. (2001). "Robust LPV control of a flexible rotor supported on magnetic bearings," *Proceedings of the 6th Int. Symp. on Magnetic Suspension Technology*, Turin, Italy, October, 2001.